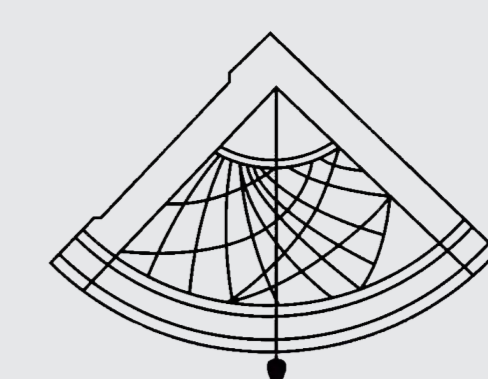


# Spatio-temporal monitoring of surface deformation of the North Anatolian Fault Zone in Düzce Region by InSAR technique

Çağkan Serhun Zoroğlu<sup>1</sup>, Tülay Kaya Eken<sup>1</sup>, Emre Havazlı<sup>2</sup>, and Haluk Özener<sup>1</sup>

<sup>1</sup>Boğaziçi University, Kandilli Observatory and Earthquake Research Institute, Geodesy, Istanbul, Türkiye, <sup>2</sup>Jet Propulsion Laboratory, California Institute of Technology, Pasadena, CA, USA

Contact: cagkan.zoroglu@boun.edu.tr



**KANDİLLİ**  
RASATHANESİ VE  
DEPREM ARAŞTIRMA  
ENSTİTÜSÜ  
1868



EGU23-833 TS3.9  
Hall X2 | X2.256  
Thu, 27 Apr, 10:45-12:30

## SUMMARY

The North Anatolian Fault Zone (NAFZ), a 1600-km-long right-lateral transform fault system of Miocene age, forms a typical plate boundary between the Anatolian and Eurasian Plates within the complex tectonic setting of the eastern Mediterranean and Anatolia, and it has generated several devastating earthquakes in the 20th century (Figure 1). The sequence of known activity along the NAFZ has begun with the 1912 M7.3 Mürefte Şarköy event along the Ganos segment at the northwestern edge of the NAFZ. Then, it moved to the furthestmost eastern segment with the 1939 M7.9 Erzincan Earthquake that appears to initiate a fairly westward migrating earthquake pattern until the 1999 Izmit-Düzce failures (Figure 2). Thus, the NAFZ has been the focus of extensive scientific attention due to its seismic hazard potential.

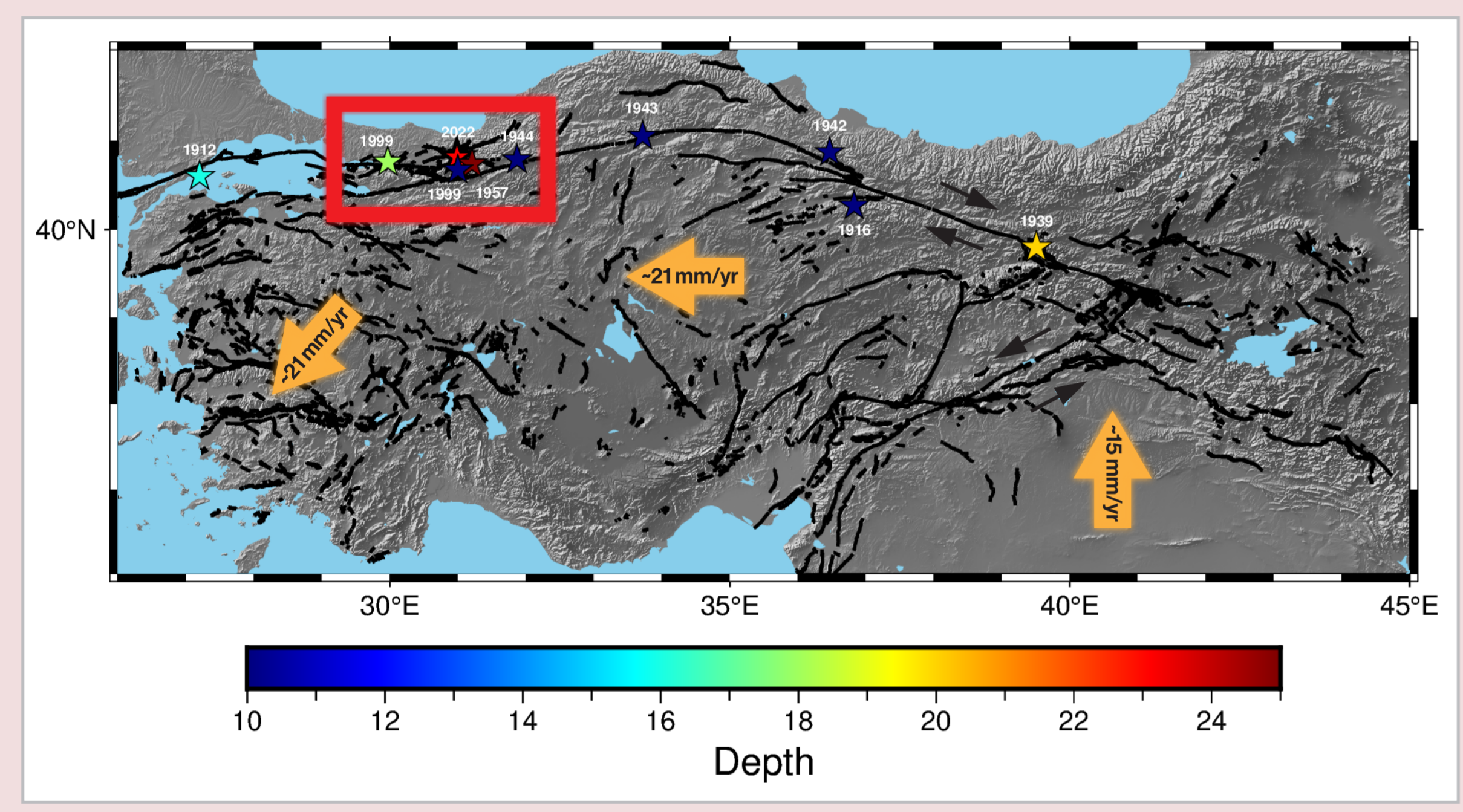


**Figure 1:** Tectonic map of Turkey showing the movement of tectonic plates (orange arrows) plotted with their plate velocities (Reilinger et al. 2006) and fault network (Emre et al. 2013). Green star represents December 27, 1939 Erzincan earthquake, orange star represents November 12, 1999 Düzce earthquake, blue star represents August 17, 1999 Izmit earthquake and red star represents November 23, 2022 Düzce earthquake.

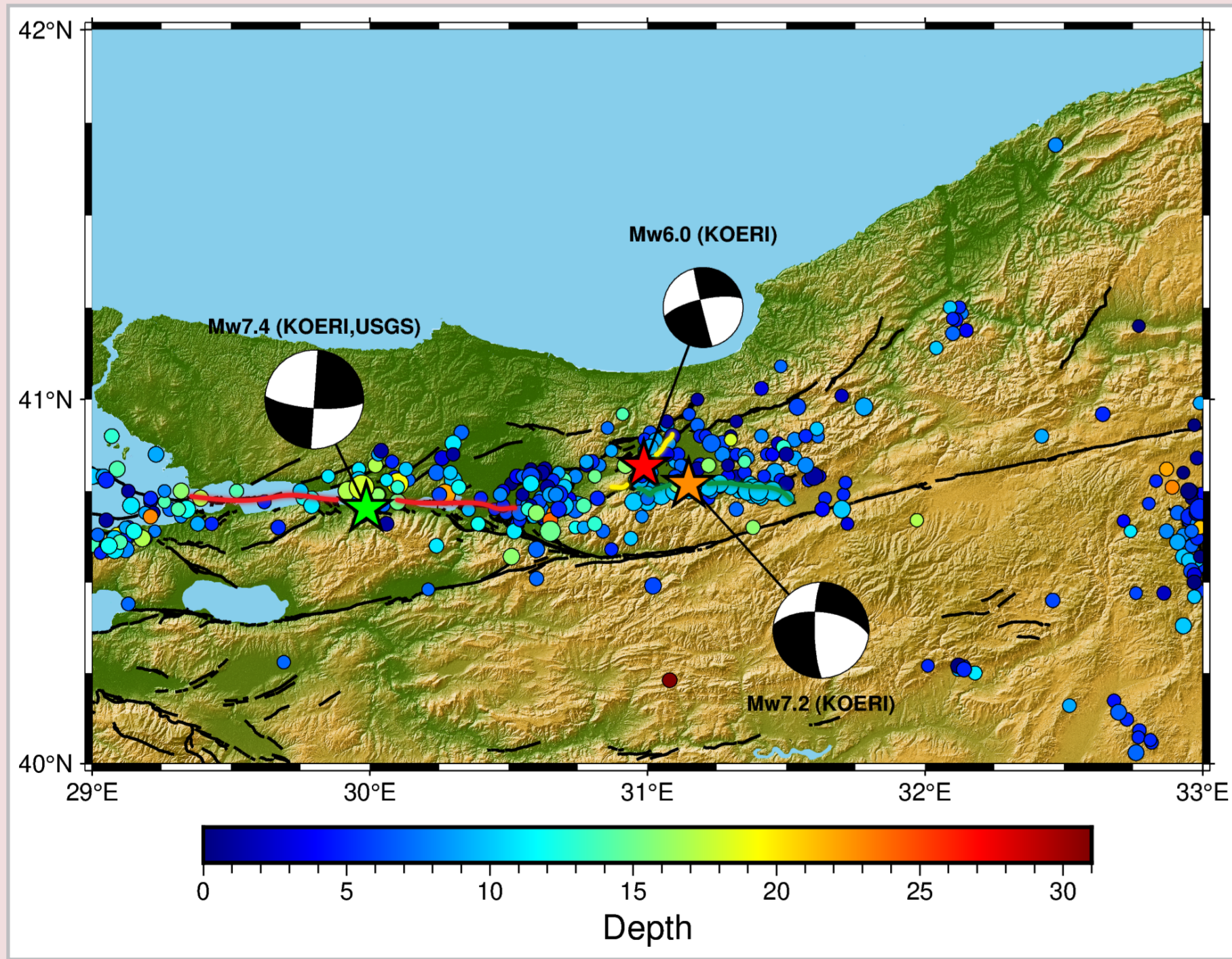


**Figure 2:** August 17, 1999 İzmit earthquake (blue star), November 12, 1999 Düzce earthquake (orange star) and November 23, 2022 Gölyaka earthquake (red star) plotted with their respective focal mechanism, their aftershocks ( $M_w \geq 3.5$ ) and fault network. Red line shows the fault rupture of the August 17, 1999 İzmit earthquake, green line shows the fault rupture of the November 12, 1999 Düzce earthquake and yellow line shows the fault rupture of the November 23, 2022 Gölyaka earthquake.

## RESISTIVITY

We select the Düzce Fault as a test case that hosted an earthquake of magnitude Mw7.2 on 1999 November 12 that struck the eastward of the 1999 August 17, Mw7.4, Izmit failure only 3 months later. Interestingly, however, Düzce failure exhibited a fault rupture character propagating with supershear and causing significant post-seismic deformation to the east of the epicenter. Early two-dimensional magnetotelluric modeling, performed along two N-S profiles located at east- and westward to the mainshock epicenter, was able to elucidate the E-W varying nature of crustal properties.

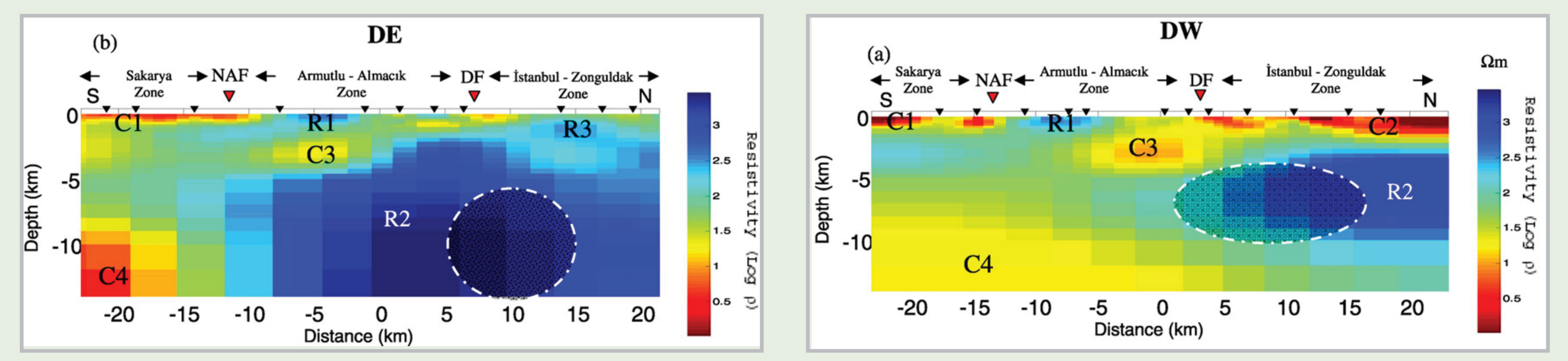


**Figure 3:** Final resistivity models for (a) DW and (b) DE profiles obtained from joint inversion of the TE and TM mode data. Black triangles at the surface represent MT stations. Red triangles indicate NAF and the Düzce fault from the south to the north, respectively. Color variation in models from red to blue denotes the increase in the resistivity. Circles including sparse and dense dots show the aftershock areas and represent sparse and dense aftershocks beneath the western and the eastern sides of the epicenter, respectively (Kaya Eken et al. 2009).

## METHOD

This study aims to determine the spatio-temporal behavior of long-term surface deformation along the Düzce Fault segment of the NAFZ. We examine the effect of physical properties of the crustal structure on the inter-seismic loading and surface creep parameters in this actively deforming area. For this purpose, we adopted the well-known InSAR timeseries method using publicly available Sentinel-1 data. Sentinel-1 observations covering our study area has a time span of 8 years between 2014 and 2022.

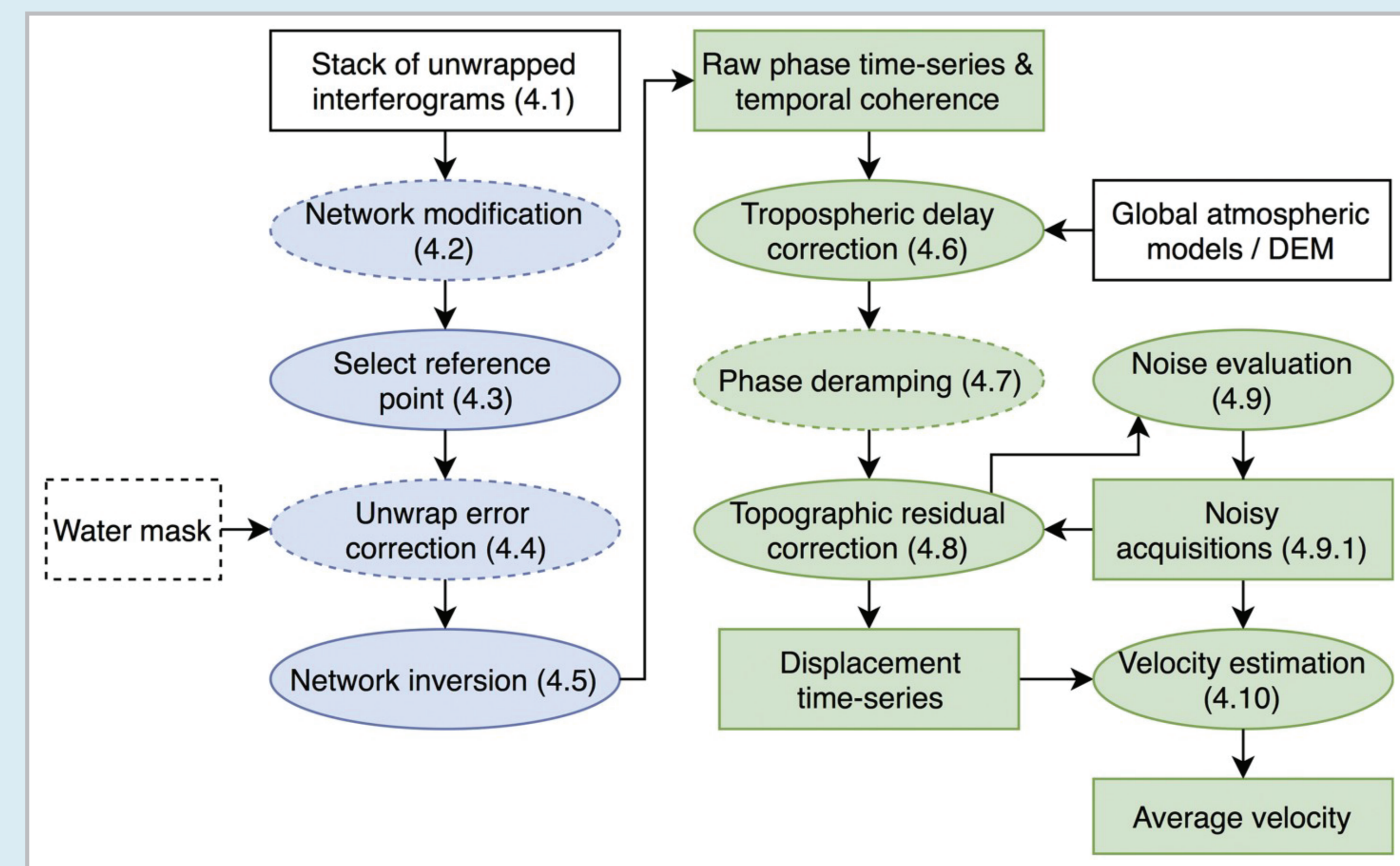


**Figure 4:** Routine process for analyzing time series using InSAR. Green ovals represent stages in the time-series domain, such as phase corrections for the tropospheric delay, phase ramps, and topographic residuals, whereas blue ovals represent processes in the interferogram domain, such as unwrapping error correction and network inversion. Rectangles in white: data input. Data output rectangles are green. Boundaries that are dashed indicate optional steps or data (Yunjun et al. 2019).

## DATA PROCESSING & RESULTS

In this study, we used Sentinel-1 data track number 65, frame number 455. We first processed the data in stackSentinel with 5 connections. Then, we processed the output of the stackSentinel with MintPy. SBAS Time Series method is used. After the process with MintPy, spatial coherence mask is applied with coherence threshold 0.4 to the geocoded velocity data. Finally, masked line of sight velocity data is plotted on the map.

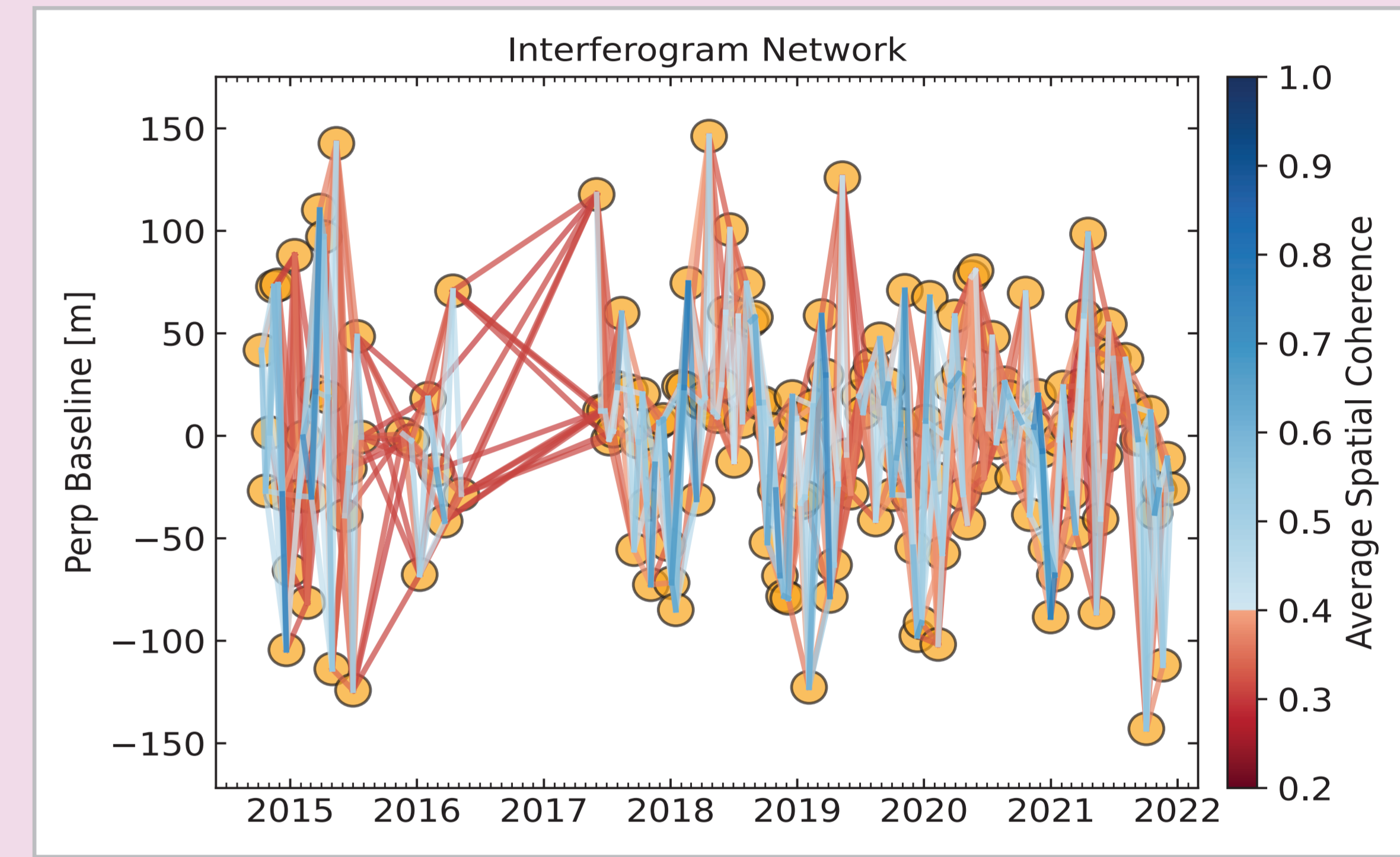


**Figure 5:** Interferogram network showing the coherence of the interferograms used in this study. Average spatial coherence mask is applied to the data with 0.4 threshold. Data before October 2015 disrupting the output excluded due to lack of coherence.

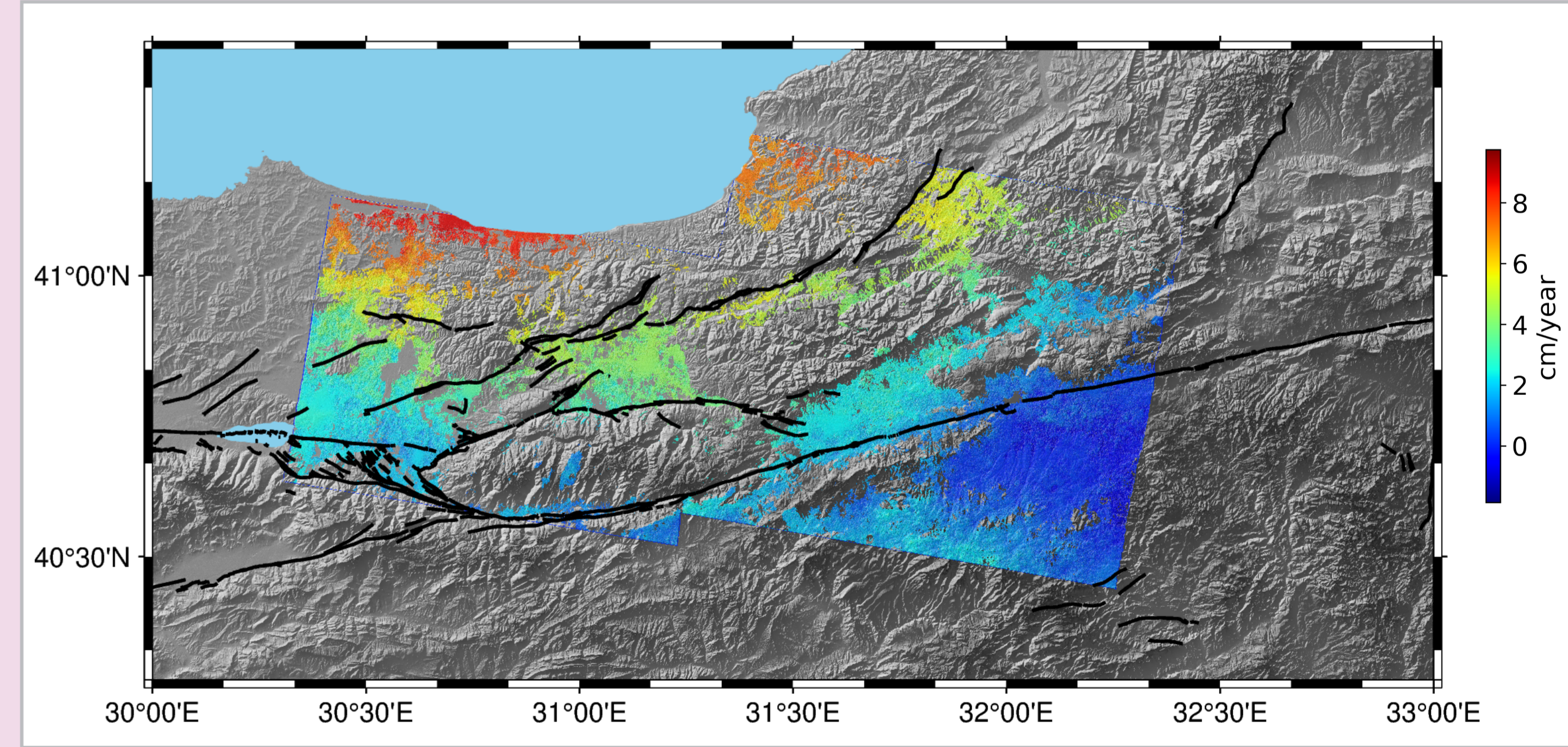


**Figure 6:** Line of sight velocity obtained from MintPy using track number 65 and frame number 455. This figure shows that the slip rate is ~30 mm/year on the Düzce fault.

## FUTURE WORKS

- Reprocess of the data from 2014 with 5 interferogram connections.
- Process of ascending data belonging to the Düzce region.
- Horizontal and vertical velocities will be obtained from combining ascending and descending data.
- Creep and locking depths for the Duzce Fault will be estimated from InSAR data.

## REFERENCES

+ Reilinger R, McClusky, S., Vernant, P., Lawrence, S., Ergintav, S., Cakmak, R., Ozener, H., Kadirov, F., Guliev, I., Stepanyan, R. et al. (2006) GPS constraints on continental deformation in the Africa-Arabia-Eurasia continental collision zone and implications for the dynamics of plate interactions. *J. Geophys. Res.*, 111, B05411. doi:10.1029/2005JB004051.  
 + Yunjun, Z., Fattahi, H., & Amelung, F. (2019). Small baseline InSAR time series analysis: Unwrapping error correction and noise reduction. *Computers & Geosciences*, 104331. doi:10.1016/j.cageo.2019.104331.  
 + Kaya, T., Tank, S. B., Tunçer, M. K., Rokoyansky, I. I., Tolak, E., & Savchenko, T. (2009). Asperity along the North Anatolian Fault imaged by magnetotellurics at Düzce, Turkey. *Earth, Planets and Space*, 61(7), 871-884. doi:10.1186/bf03353198  
 + Emre, Ö., Duman, T.Y., Özalp, S., Elmacı, H., Olgun, Ş. and Şaroglu, Ş., 2013. Active fault map of Turkey with explanatory text. Ankara: General Directorate of Mineral Research and Exploration, Special Publication Series-30.